Life Sciences 276 (2021) 119399

Contents lists available at ScienceDirect

Life Sciences

journal homepage: www.elsevier.com/locate/lifescie

Exosomal miR-4443 promotes cisplatin resistance in non-small cell lung carcinoma by regulating FSP1 m6A modification-mediated ferroptosis

Zhiyu Song [a,*], Gang Jia [b], Peizhi Ma [a], Shundong Cang [b]

[a] Department of Pharmacy, Henan Provincial People's Hospital, People's Hospital of Zhengzhou University, Zhengzhou, Henan 450003, China
[b] Department of Oncology, Henan Provincial People's Hospital, People's Hospital of Zhengzhou University, Zhengzhou, Henan 450003, China

ARTICLE INFO

Keywords:
Exosome, cisplatin resistance
NSCLC
FSP1, ferroptosis
m6A modification

ABSTRACT

Aims: Exosomal transfer of miRNAs affects recipient cell proliferation and chemoresistance. Here, we aimed to investigate the role of exosomal miRNAs in controlling cisplatin resistance in non-small cell lung carcinoma (NSCLC).

Main methods: Paired tumor and normal tissue-derived exosomes were collected from NSCLC patients with low or high responsiveness to cisplatin treatment. The results showed that the microRNA-4443 (miR-4443) level was upregulated in cisplatin-resistant NSCLC tumor tissue-derived exosomes compared with cisplatin-sensitive tissue-derived exosomes. Cisplatin-resistant cells (A549-R) were generated from the parental cells (A549-S). Resistant exosomes conferred cisplatin resistance by transferring miR-4443 to sensitive cells. Moreover, overexpression of miR-4443 inhibited FSP1-mediated ferroptosis induced by cisplatin treatment *in vitro* and enhanced tumor growth *in vivo*.

Key findings: Through bioinformatics analysis and luciferase assays, METTL3 was confirmed as a direct target gene of miR-4443. Further mechanistic analysis showed that miR-4443 regulated the expression of FSP1 in an m6A manner *via* METLL3.

Significance: Our findings provide more in-depth insight into the chemoresistance of NSCLC and support the therapeutic potential of targeting ferroptosis.

1. Introduction

Lung cancer is a leading cause of cancer-related death worldwide. Non-small cell lung cancer (NSCLC), which includes lung adenocarcinoma, lung squamous cell cancer, and large cell carcinoma, is the major type of lung cancer [1]. Important advancements in NSCLC treatment have shown compelling clinical benefits, achieving early detection and improved care [2]. However, the overall survival rate is limited, specifically for patients with metastasis. Currently, platinum-based chemotherapy, including cisplatin and carboplatin, is still the first-line treatment for NSCLC [3]. Cisplatin covalently binds to DNA, forming DNA adducts, and consequently activates various signal transduction pathways involved in cell cycle arrest, DNA damage recognition and repair, and programmed cell death. Cisplatin can induce several forms of cell death, including pyroptosis, apoptosis, ferroptosis, and autophagy. Recently, cisplatin was proven to induce ferroptosis and apoptosis in NSCLC [4]. Treating NSCLC patients with cisplatin showed benefits; however, this treatment could not sustainably prolong overall survival in elderly patients due to severe side effects, and the effects could be suppressed by resistance associated with relapse and poor quality of life [5–7]. Therefore, further elucidation of the underlying mechanisms and identification of novel strategies are required to improve cisplatin sensitivity and outcomes in NSCLC.

Exosomes are small vesicles approximately 50–150 nm in diameter. They are released by almost all cell types and play a key role in cell-cell communication by transferring abundant molecular components, such as proteins, RNAs, and even lipids [8,9]. Recently, emerging evidence revealed that cancer cells release exosomes into the tumor microenvironment, altering the chemotherapy resistance of recipients [10]. To date, exosomal miRNAs have been reported as crucial indicators for multiple cancer types, including NSCLC [11,12]. For instance, Liu et al. discovered that exosomes derived from gemcitabine-resistant tumor cells could be internalized by recipient cells and reduced the sensitivity of these cells to gemcitabine treatment by transferring miR-222-3p [13]. Similarly, Shen et al. reported that a high level of exosomal miR-425-3p was associated with chemoresistance, which might facilitate malignant

* Corresponding author.
E-mail address: song545669744@163.com (Z. Song).

https://doi.org/10.1016/j.lfs.2021.119399
Received 3 December 2020; Received in revised form 8 March 2021; Accepted 16 March 2021
Available online 27 March 2021

characteristics in sensitive tumor cells [14]. Interestingly, miR-4443 has been identified as a key regulator of tumorigenesis and metastasis [15–18]. A previous study reported that miR-4443 expression was dramatically upregulated in NSCLC patients with resistance to epirubicin chemotherapy, and this molecule reduced cell apoptosis and cell cycle arrest by activating the JAK2/STAT3 pathway [19]. Moreover, Qin et al. profiled the miRNA expression levels between cisplatin-resistant cells and their parental cells using the NSCLC cell line A549. In their study, a total of 11 upregulated miRNAs and 31 downregulated miRNAs were significantly different between cisplatin-resistant A549 cells and parental cells, as well as between cisplatin-resistant A549 cell-derived exosomes and A549 cell-derived exosomes. Among these miRNAs, miR-4443 was the top upregulated miRNA in cisplatin-resistant A549 cell-derived exosomes [20], yet little is known about the role of miR-4443 in NSCLC resistance to cisplatin treatment.

In this study, we explored the exosomal miR-4443 expression pattern in clinical NSCLC samples and NSCLC cell lines. Moreover, we discussed the relationship between miR-4443 and the chemoresistance of NSCLC to cisplatin. We found that miR-4443 was enriched in exosomes derived from both cisplatin-resistant clinical NSCLC samples and cisplatin-resistant NSCLC cell lines. Moreover, functional studies showed that exosomal miR-4443 could promote cell resistance to cisplatin in NSCLC *via* FSP1 m6A-mediated ferroptosis. Our findings revealed the function of miR-4443 in the chemotherapy response and provided a novel biomarker to predict the efficacy of cisplatin treatment for patients with NSCLC.

2. Materials and methods

2.1. Clinical samples

Fresh NSCLC tumor tissue and normal lung tissue samples from patients were obtained from the People's Hospital of Zhengzhou University. All patients were diagnosed with NSCLC and previously treated with cisplatin-based chemotherapy. This experiment was approved by the People's Hospital of Zhengzhou University, and written informed consent was obtained from all patients.

2.2. Exosome isolation and identification

Exosomes derived from tumor and normal lung tissues were isolated as described previously [21]. Briefly, small pieces of these tissues were homogenized gently using 75 U/mL collagenase at 37 °C for 1 h. The tissues were then centrifuged at 300 ×g for 5 min at 4 °C. The supernatants were collected and centrifuged at 2000 ×*g* for 15 min, 10,000 ×g for 30 min, and 100,000 ×g for 4 h at 4 °C, followed by purification using a sucrose cushion. Subsequently, the exosomes were washed with PBS and resuspended in 200 μL of PBS for further study. For cell-derived exosome isolation, A549-S (the parental A549 cells) or A549-R cells were cultured in culture medium containing 10% exosome-free FBS (Thermo, USA) for 48 h. The conditioned medium was collected and subjected to series centrifugation as described above.

Exosomes were embedded, cut and observed under a transmission electron microscope (TEM) (JEM-2100F, Japan) as described in a previous study [22]. In addition, the size distribution of exosomes was measured using a NanoSight NS300 system (NTA, Malvern Instruments, China) following the manufacturer's instructions. Furthermore, biomarkers of exosomes, including CD63 (1:1000, Abcam, USA), CD81 (1:1000, Abcam, USA), CD9 (1:1000, Abcam, USA) and Alix (1:1000, Abcam, USA), were detected by western blots. For determination of whether exosomes could be taken up by recipients, the pellets were dyed with PKH67 dye (Beyotime, China) for 1 h at room temperature. After incubation with A549-S cells for 6 h, labeled exosomes were visualized under a confocal microscope (FV1000, Olympus, Japan) using a 488 nm laser. For exosome treatment, A549-S cells were incubated with 20 ng/mL exosomes (in 100 μL of PBS) derived from cisplatin-resistant tumor tissues for 48 h.

2.3. Cell culture

The HEK293T, 16HBE, PGCL3, H460, H1299, and A549 cell lines were obtained from ATCC (Manassas, USA) and cultured with DMEM culture medium (Gibco, USA) supplemented with 10% fetal bovine serum (Gibco, USA) and 1% penicillin and streptomycin (Thermo, USA). For generation of cisplatin-resistant A549 cells (A549-R), parental A549 cells (A549-S) were treated with cisplatin at 10% of the IC_{50} dose and gradually increasing doses in subsequent passages. The A549-R cells were maintained in medium containing 1 μg/mL cisplatin (Sigma, USA).

2.4. Quantitative reverse transcription polymerase chain reaction (qRT-PCR)

According to the manufacturer's instructions, total RNA was extracted from the cells and exosomes using TRIzol reagent (Thermo, USA). Next, 1 μg of total RNA was reverse-transcribed to cDNA using the TaqMan Reverse Transcription Kit or TaqMan microRNA Reverse Transcription Kit (Applied Biosystems, USA). Subsequently, qRT-PCR was performed to detect the expression of genes and miRNAs using SYBR Green (Toyobo, Japan). The results were obtained using the $2^{-\Delta\Delta CT}$ method and normalized with U6 or GAPDH. The primers used in this study were as follows: miR-4443 (human): forward 5′-GCGCGTTGGAGGCGTG-3′, reverse 5′-AGTGCAGGGTCCGAGGTATT-3′; METTL3 (human): forward 5′-GTCCGCGTGAGAATTGGCTA-3′, reverse 5′-CGTCCGTCCGGTAAAAGTGA-3′; *FSP1* (human): forward 5′-CGTCTACGCCATTGGTGACT-3′, reverse 5′-TGGGATAGCCCAAAAAGGCT-3′; GAPDH (human): forward 5′-AAGGGCCCTGACAACTCTTTT-3′, reverse 5′-CTGGTGGTCCAGGGGTCTTA-3′; U6 (human): forward 5′-GAAGCGCGGCCACGAG-3′, reverse 5′-AGTGCAGGGTCCGAGGTATT-3′.

2.5. Cell transfection

The miR-4443 inhibitor, mimic and related controls (mimic-NC, inhibitor-NC), METTL3 overexpression and knockdown vectors (METTL3-OE, METTL3-KD), FSP1 overexpression and knockdown vectors (FSP1-OE, FSP1-KD) and the empty vector were obtained from GenePharma (Shanghai, China). For *in vitro* transfection, the cells were plated on 6-well plates at a density of 10^6 cells per well. Next, the cells were transfected with these reagents (5 μg of all) using Lipofectamine 2000 following the manufacturer's instructions. After 48 h, the cells were used for further studies.

2.6. CCK-8 assay and colony formation assay

Cells were plated on 96-well plates (5000 cells/well). After treatment with 5 μg/mL cisplatin (Sigma, USA) for 0 h–96 h, 10 μL of CCK-8 (Dojindo, Japan) solution was added per well and incubated at 37 °C for 2 h. The optical density was detected by a microplate reader at 450 nm. For the colony formation assays, 1000 cells were seeded into 6-well plates and treated with 5 μg/mL cisplatin for 24 h. Subsequently, the cells were maintained in fresh medium for 7 days. The colonies were fixed with methanol, stained with hematoxylin and observed using a light microscope.

2.7. Cell treatment

A549-S cells were exposed to multiple reagents to evaluate ferroptosis-induced cell death. The dose and conditions of these reagents were as follows: cisplatin was dissolved in PBS at a final working concentration of 5 μg/mL; erastin (Selleck, China) was diluted using DMSO and added to cells at a dose of 10 μmol/L; 0.5 μmol/L ferrostatin-1 (in DMSO, Sigma, USA) or 50 μmol/L deferoxamine (in DMSO, Sigma, USA) was used; Z-VAD-FMK (20 μmol/L in DMSO, Beyotime, China),

necrostatin-1 (30 μmol/L in DMSO, Santa, USA) and chloroquine (5 μg/mL in DMSO, Meilunbio, China) were used to treat cells. After 24 h of incubation with these reagents, the cells were subjected to CCK-8 assays to detect cell viability.

2.8. Iron assay

Cells were collected to determine the intracellular ferrous iron level using an iron assay kit (Abcam, USA). Briefly, after the samples were washed with PBS several times, they were homogenized and incubated with an iron reducer on ice for 30 min, followed by incubation with the iron probe for 1 h. The output was measured by a microplate reader (Bio-Tek, USA) at 593 nm.

2.9. Reactive oxygen species (ROS) detection

For lipid ROS detection, the cells were seeded on 6-well plates (10^6 cells/well) and subjected to different treatments. After the cells were washed with PBS, they were stained using CellRox Green reagent (5 μM, Thermo, USA) for 30 min. Nuclei were stained with 4,6-diamidino-2-phenylindole (DAPI). The images were observed under a fluorescence microscope (Zeiss, Germany).

2.10. Intracellular superoxide detection

After different treatments, the cells (10^6 cells/well) were incubated with 5 μM MitoSOX-Red (Invitrogen, USA) for 20 min at 37 °C and stained for DAPI as described above. The images were observed under a fluorescence microscope (Zeiss, Germany).

2.11. Western blot

Cells were harvested after different treatments and homogenized using RIPA buffer. Equal total proteins (30 μg/lane) were loaded and separated by SDS-PAGE (Bio-Rad, USA). The proteins were transferred onto PVDF membranes and blocked with 5% BSA for 2 h at room temperature. Next, the membranes were incubated with primary antibodies against FSP1 (1:1000, Abcam, USA), METTL3 (1:1000, Abcam, USA) and GAPDH (1:5000, Abcam, USA) at 4 °C overnight, followed by incubation with HRP-conjugated secondary antibodies (1:5000, Abcam, USA) for 2 h at room temperature. The bands were then developed using enhanced chemiluminescence chromogenic substrate (GE Healthcare, UK) and analyzed by ImageJ software. GAPDH was used as a control in this study.

2.12. Luciferase assay

The 3′-UTR of METTL3 was cloned into the pmiR-RB-REPORT vector (RiboBio, China). The binding sites were mutated using a site-directed mutagenesis kit (NEB E0554, USA). HEK293T cells were maintained in 6-well plates (10^6 cells/well) and cotransfected with vectors containing the wild-type or mutant 3′-UTR of METTL3 and miR-4443 mimic, inhibitor and related controls using Lipofectamine 2000 reagent. After 48 h, luciferase activity was detected using a Dual-Luciferase Assay System (Promega, USA) according to the manufacturer's instructions.

2.13. m6A RNA methylation quantification

The content of m6A in total RNA was assessed using m6A RNA Methylation Quantification Kit (Abcam, USA) following the manufacturer's instructions. Briefly, total RNA was mixed with RNA high binding solution and incubated with the specific capture antibody and detection antibody. Finally, the m6A signal was developed using the enhancer and color developing solutions, followed by detection using a microplate reader at 450 nm.

2.14. MeRIP-qPCR assay

MeRIP-qPCR was performed according to previous studies [23,24]. The purified total mRNA (100 μg) was isolated and incubated with 2 μg m6A antibody (Abcam, USA) or normal rabbit IgG (Abcam, USA) and 20 μL of SureBeads protein A/G mixed magnetic beads (Bio-Rad, USA) at 4 °C overnight. The RNAs were then eluted with 200 μL of 0.5 mg/mL N^6-methyladenosine 5-monophosphate sodium salt for 1 h at 4 °C, followed by qRT-PCR analysis.

2.15. Animal experiment

The animal experiments were approved by the Ethics Committee of People's Hospital of Zhengzhou University. BALB/c nude mice (male, 4 weeks old) were purchased from the Animal Center of Nanjing University with free access to water and food. A549 cells (10^6 cells per mouse) transfected with miR-4443 mimic or mimic-NC were injected subcutaneously to generate subcutaneous tumors. Tumor volume was recorded and measured according to the formula as follows: tumor volume = (length × width^2) / 2. Once the volume reached 100 mm^3, the mice were treated with cisplatin (5 mg/kg in PBS) or PBS *via* intraperitoneal injection. Tumor volume was measured every five days after cisplatin treatment. Finally, the tumor tissues were removed for weighing and further studies when the mice were sacrificed.

2.16. H&E staining and immunohistochemistry (IHC) assay

Tumor tissues were collected and fixed with a 10% formaldehyde solution. The tissues were then embedded in paraffin and cut into 5 μm sections. The sections were stained with an H&E staining kit (Beyotime, China) according to the manufacturer's instructions. For the IHC assay, the sections of tumor tissues or normal lung tissues were deparaffinized, rehydrated and heated in a water bath for antigen retrieval. After the sections were blocked with 1% bovine serum albumin for 2 h at room temperature, they were incubated with antibodies against METTL3 (1:400, Abcam, USA), FSP1 (1:400, Abcam, USA) and Ki-67 (1:400, Abcam, USA) overnight at 4 °C, followed by visualization using the Dako Real EnVision Inspection System (Dako, Denmark). The images were observed under a light microscope (Nikon, Japan).

2.17. Statistical analysis

Data were analyzed using Prism 8.0 software and are shown as the mean ± SD. Two-tailed Student's *t*-test was used to compare two groups. One-way ANOVA was used for comparisons among multiple groups. $p < 0.05$ was considered statistically significant.

3. Results

3.1. miR-4443 is enriched in exosomes of cisplatin-resistant NSCLC tumors

Tumor-derived exosomal miRNAs can be used as specific biomarkers of prognosis and diagnosis. In this study, we first examined the expression levels of tumor tissue-derived exosomal microRNAs from NSCLC patients with low or high responsiveness to cisplatin treatment. Based on the progression-free survival time, the samples were divided into cisplatin-resistant (PFS < 6 months) and cisplatin-sensitive (PFS > 6 months) NSCLC. Exosomes were isolated from tumor tissues and normal tissues and characterized by transmission electron microscopy and NTA analysis. As shown in Fig. 1A and B, tissue-derived vesicles displayed a round structure approximately 100 nm in diameter, and all four positive protein markers of exosomes, CD63, CD81, CD9, and Alix, were expressed in these vesicles, indicating that we successfully obtained exosomes (Fig. 1C). Next, the expression levels of miR-4443 in normal tissue and cisplatin-sensitive (Cis—S) and cisplatin-resistant (Cis-R)

tumor tissues were monitored using qRT-PCR. Compared with that of the control, the mean expression level of miR-4443 was approximately 3-fold lower in the Cis-S samples and approximately 1.5-fold higher in the Cis-R samples (Fig. 1D). In addition, we profiled the expression levels of miR-4443 in a panel of NSCLC cell lines, such as A549 (denoted as A549-S in this article), NCL—H1299, NCL-H460 and PGCL3, as well as cisplatin-resistant A549 (A549-R) and H460 (H460-R) cells. The results showed that miR-4443 was significantly upregulated in A549-R cells and H460-R cells compared with normal bronchial epithelial cells (16HBE) (Figs. 1E, S1). miR-4443 expression was approximately 15 times higher in exosomes derived from A549-R cells than in exosomes derived from A549-S cells (Fig. 1F), similar to the results in clinical samples (Fig. 1D). Therefore, we used the A549 cell line for further study.

3.2. Exosomal miR-4443 induces cisplatin resistance in A549 cells

To explore the effect of miR-4443 in tumor exosomes on the responsiveness to cisplatin treatment, we cocultured A549-S cells with exosomes released by fresh NSCLC tumor tissues from patients of similar ages. All these patients were diagnosed with NSCLC and previously treated with cisplatin-based chemotherapy. Exosomes from those who were sensitive or resistant to cisplatin treatment were labeled Cis-S and Cis-R, respectively. As shown in Fig. 2A, we observed that these exosomes could be taken up by A549-S cells, as evidenced by a clear green signal (PKH67) inside the recipient cells. In addition, Cis-R-derived

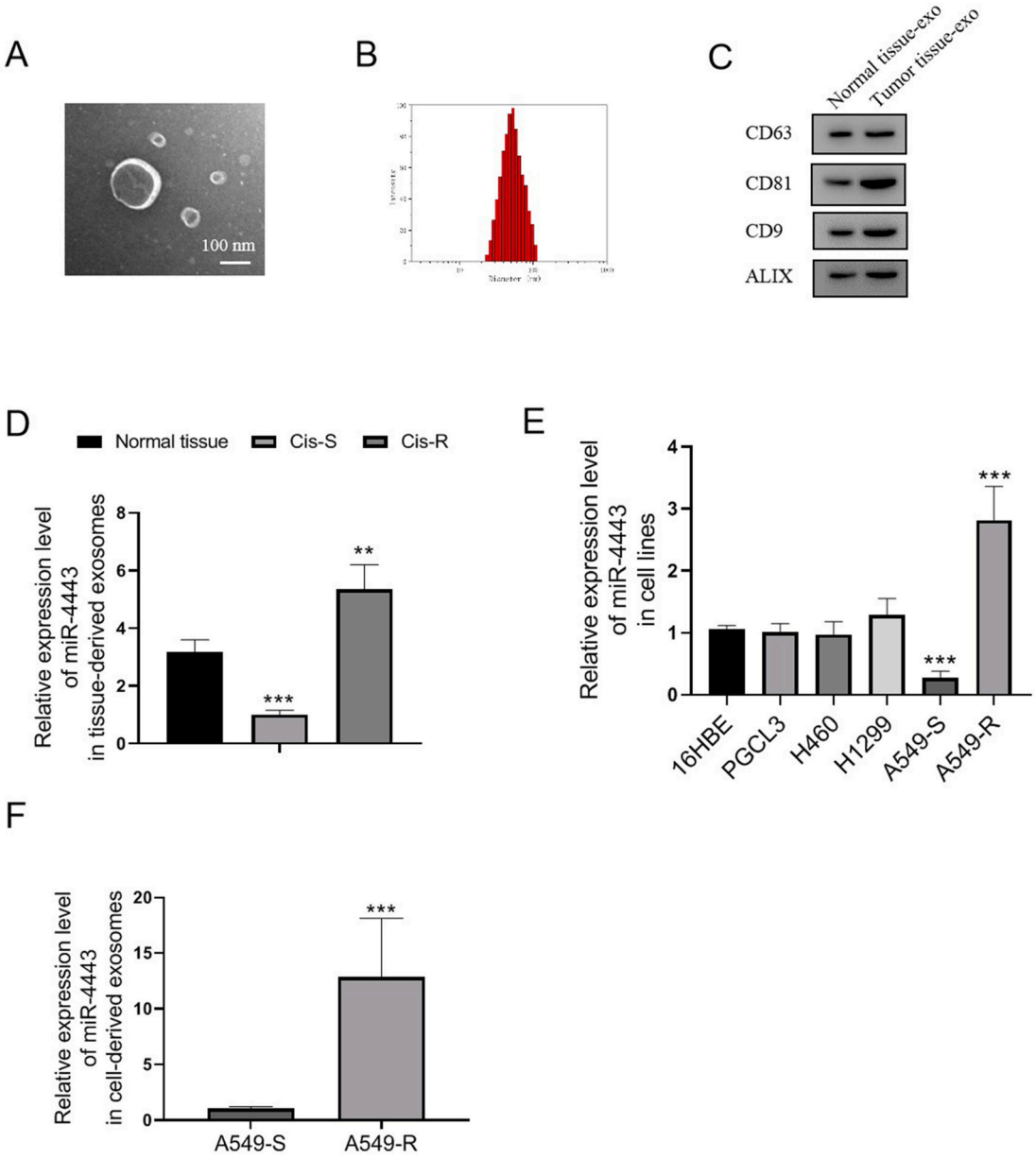

Fig. 1. miR-4443 expression is increased in cisplatin-resistant tissues and cell-derived exosomes. A. A representative image of the transmission electron micrograph is presented for the tumor tissue-derived exosomes. Bar = 100 nm. B. The size of tumor tissue-derived exosomes was determined using NanoSight particle tracking analysis (NTA). C. Representative blots were performed to determine the expression of CD63, CD81, CD9, and Alix in normal tissue and tumor tissue-derived exosomes. D. The expression of exosomal miR-4443 from cisplatin-sensitive tumor (Cis-S), cisplatin-resistant tumor (Cis-R) and normal lung tissues was detected by qRT-PCR. $^{**}p < 0.01$, $^{***}p < 0.001$ *vs.* the normal tissue group. E. The expression of miR-4443 in NSCLC cells (PGCL3, H460, H1299, A549-S, and A549-R) and normal cells (16HBE) was detected by qRT-PCR. $^{***}p < 0.001$ *vs.* the 16HBE cell group. F. The abundance of exosomal miR-4443 derived from A549-S and A549-R cells was evaluated by qRT-PCR. $^{***}p < 0.001$ *vs.* the A549-S cell group. Data are presented as the mean ± SD of three independent experiments.

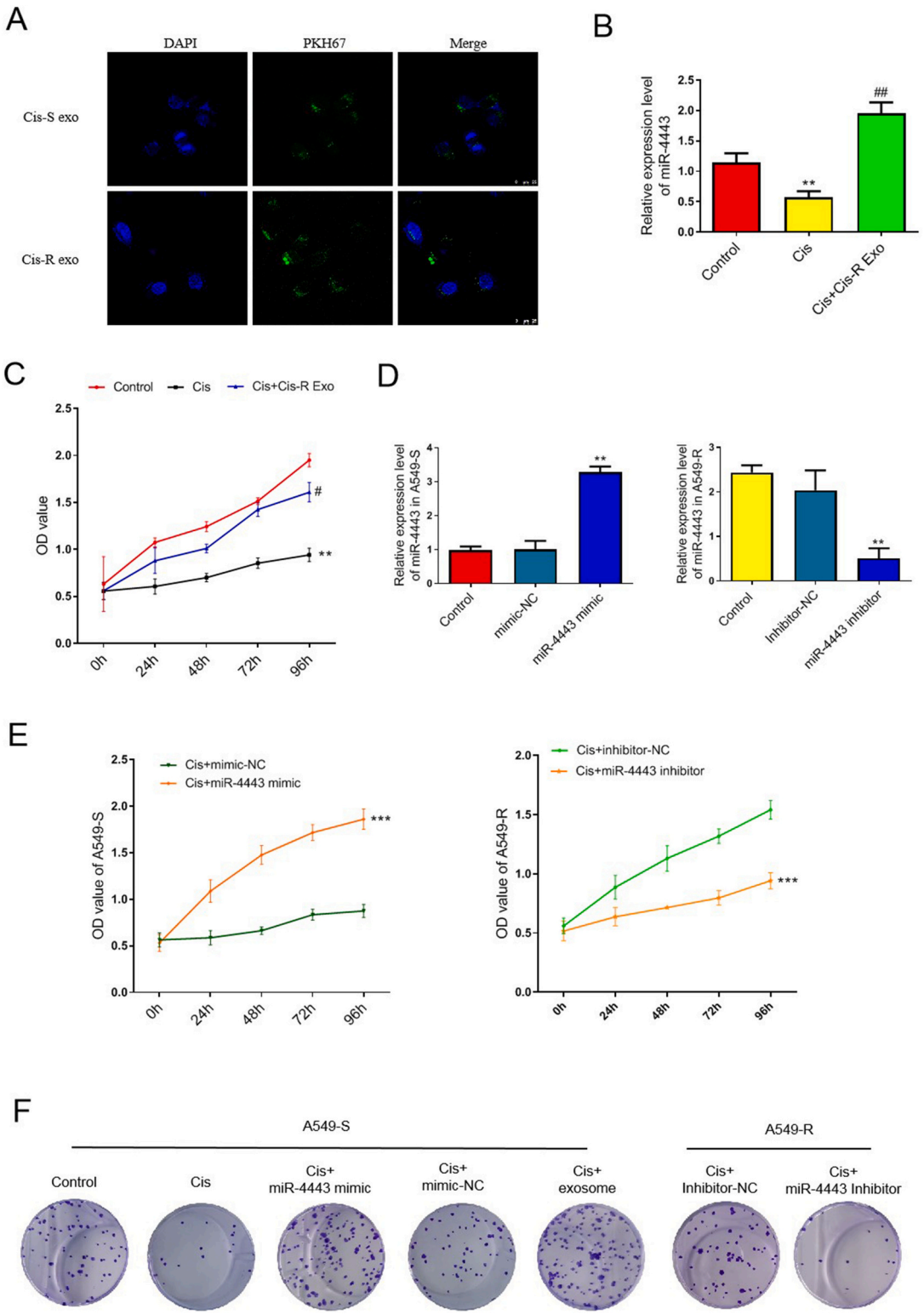

Fig. 2. Exosomal miR-4443 induces cisplatin resistance in recipient cells. A. Representative confocal microscopy images showing exosome internalization in A549-S cells after coincubation with PKH67-labeled exosomes derived from cisplatin-resistant or cisplatin-sensitive tumor tissues. The nuclei were stained by DAPI. Bar = 25 μm. B and C. After coincubation with exosomes from Cis-R for 48 h and then cisplatin treatment for 0–96 h, the level of miR-4443 in the A549-S cells and the cell viability were assessed by qRT-PCR and CCK-8 assays, respectively. The control cells were treated with an equal volume of PBS. $^{**}p < 0.01$ *vs.* the control group; $\#p < 0.05$, $\#\#p < 0.01$ *vs.* the cisplatin-treated group. D. After incubation with miR-4443 mimic, inhibitor and related controls (mimic-NC, inhibitor-NC), the levels of miR-4443 in A549-S and A549-R cells were detected by qRT-PCR. The control group was untreated. $^{**}p < 0.01$ *vs.* the mimic-NC or inhibitor-NC group. E. The viability of A549-S and A549-R cells was assessed by CCK-8 assays after different transfections and treatment with 5 μg/mL cisplatin for 0–96 h. $^{***}p < 0.001$ *vs.* the related control group (cis + mimic-NC, cis + inhibitor-NC). F. Cell proliferation of A549-S or A549-R cells after different treatments was analyzed by colony assays. Data are presented as the mean ± SD of three independent experiments.

exosomes significantly increased the miR-4443 expression level and significantly reversed the reduction in cell viability induced by cisplatin treatment (Fig. 2B and C). Moreover, gain- and loss-of-function experiments of miR-4443 expression in A549 cells were performed. The results showed that miR-4443 expression was upregulated significantly in the miR-4443 mimic-transfected A549-S cells, whereas expression of this microRNA was dramatically downregulated in the A549-R cells transfected with miR-4443 inhibitor (Fig. 2D). Ectopic expression of miR-4443 dramatically decreased the sensitivity of A549-S cells, while silencing of miR-4443 expression using an inhibitor significantly sensitized A549-R cells to cisplatin compared with the related control group (cis + inhibitor-NC, Fig. 2E). A similar trend was also observed in the colony assay upon the same treatments (Fig. 2F). These findings indicated that miR-4443 in exosomes could alter the cisplatin resistance of recipient cells.

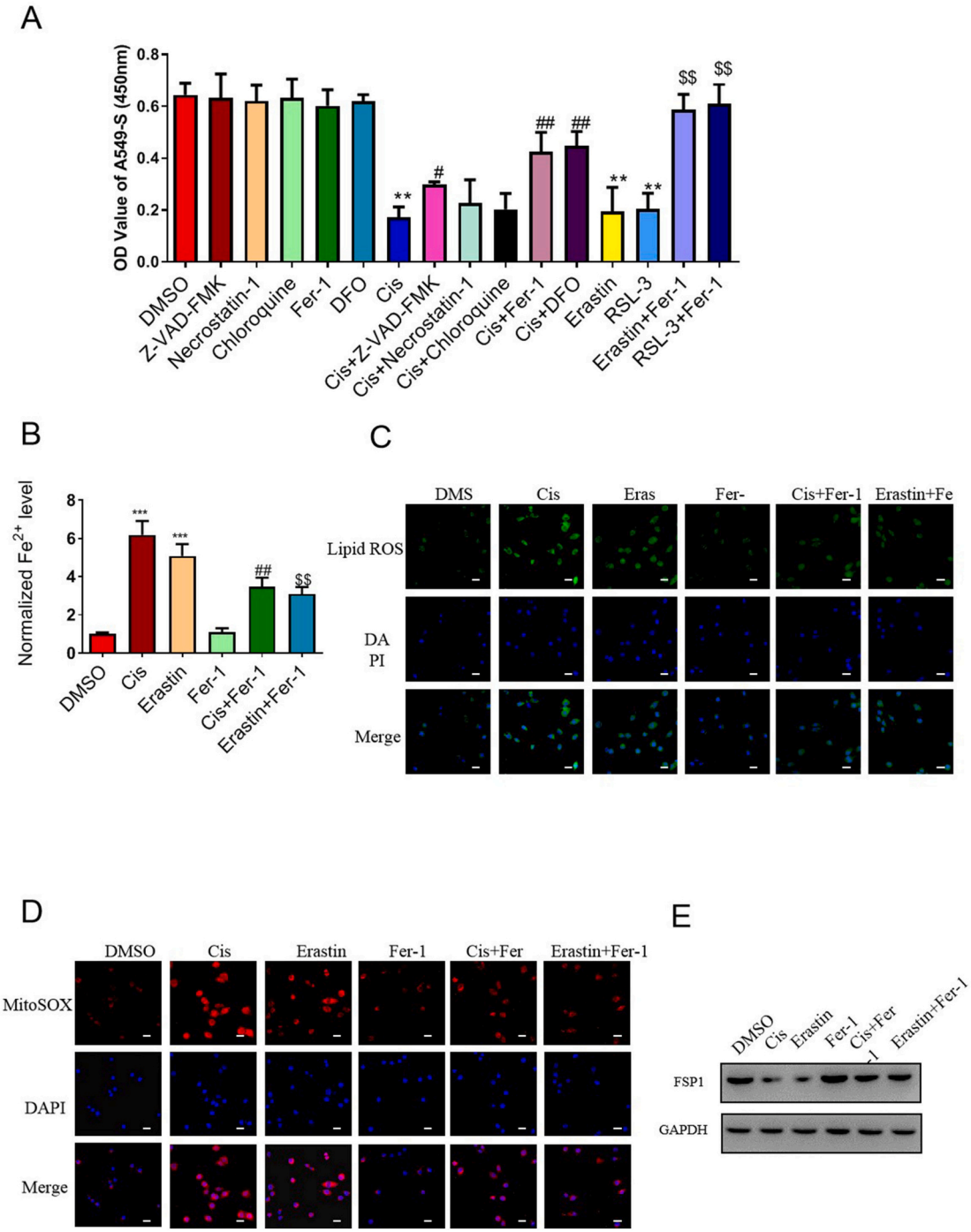

Fig. 3. Cisplatin induces ferroptosis of A549-S cells. A. A549-S cells received different treatments for 24 h. Cell viability was determined by CCK-8 assays. **p < 0.01 *vs.* the DMSO group; #p < 0.05, ##p < 0.01 *vs.* the cisplatin-treated group; $$p < 0.01 *vs.* the erastin- or RSL-3-treated group. B. A549-S cells received cisplatin, erastin, Fer-1, cisplatin + Fer-1 or erastin + Fer-1 treatments for 24 h. Iron accumulation was determined by iron assays. ***p < 0.001 *vs.* the DMSO group; ##p < 0.01 *vs.* the cisplatin-treated group; $$p < 0.01 *vs.* the erastin-treated group. C and D. The lipid ROS and MitoSOX levels in the A549-S cells after different treatments were analyzed. Bar = 20 μm. E. Representative blots showing the expression of FSP1 in A549-S cells after different treatments. Data are presented as the mean ± SD of three independent experiments.

3.3. Cisplatin inhibits tumor proliferation by inducing cell ferroptosis

As a potent antitumor agent in the clinic, cisplatin works mainly by inducing DNA lesions and programmed cell death in tumor cells. In this study, 24 h of cisplatin treatment markedly induced cell death in A549-S cells compared with that of the DMSO group (Fig. 3A). Cisplatin can cause several forms of cell death, including pyroptosis, apoptosis, ferroptosis, and autophagy [25–27]. To determine which is the major mechanism of cell death during cisplatin treatment, we used different inhibitors, such as Z-VAD-FMK (apoptosis inhibitor), necrostatin-1 (necrosis inhibitor), chloroquine (autophagy inhibitor), ferrostatin-1 and deferoxamine (Fer-1, DFO, two ferroptosis inhibitors), to treat A549-S cells. The results showed that although cisplatin-induced cell death could be reversed by both the apoptosis inhibitor Z-VAD-FMK and the ferroptosis inhibitors Fer-1 and DFO, the latter showed a stronger effect (Figs. 3A, S2). To verify whether ferroptosis is a major mechanism of cell death caused by cisplatin-treated A549-S cells, we added the ferroptosis inducers erastin and RSL-3 to the culture medium. These inducers significantly reduced cell viability compared with that of the DMSO group, and this reduction was abolished with the addition of Fer-1, a ferroptosis inhibitor (Fig. 3A). Furthermore, both cisplatin and erastin effectively increased the ferrous iron content, intracellular superoxide level and ROS accumulation in A549-S cells, and these effects were significantly reversed by Fer-1 (Fig. 3B, C and D). Consistently, western blot analysis indicated that cisplatin inhibited the expression of FSP1, which is an essential ferroptosis suppressor. A combination of cisplatin and Fer-1 re-increased FSP1 expression. A similar trend was observed when cells were cotreated with erastin and Fer-1 (Fig. 3E). These findings confirmed that ferroptosis was the main form of cell death induced by cisplatin; therefore, we investigated whether miR-4443 plays a role in

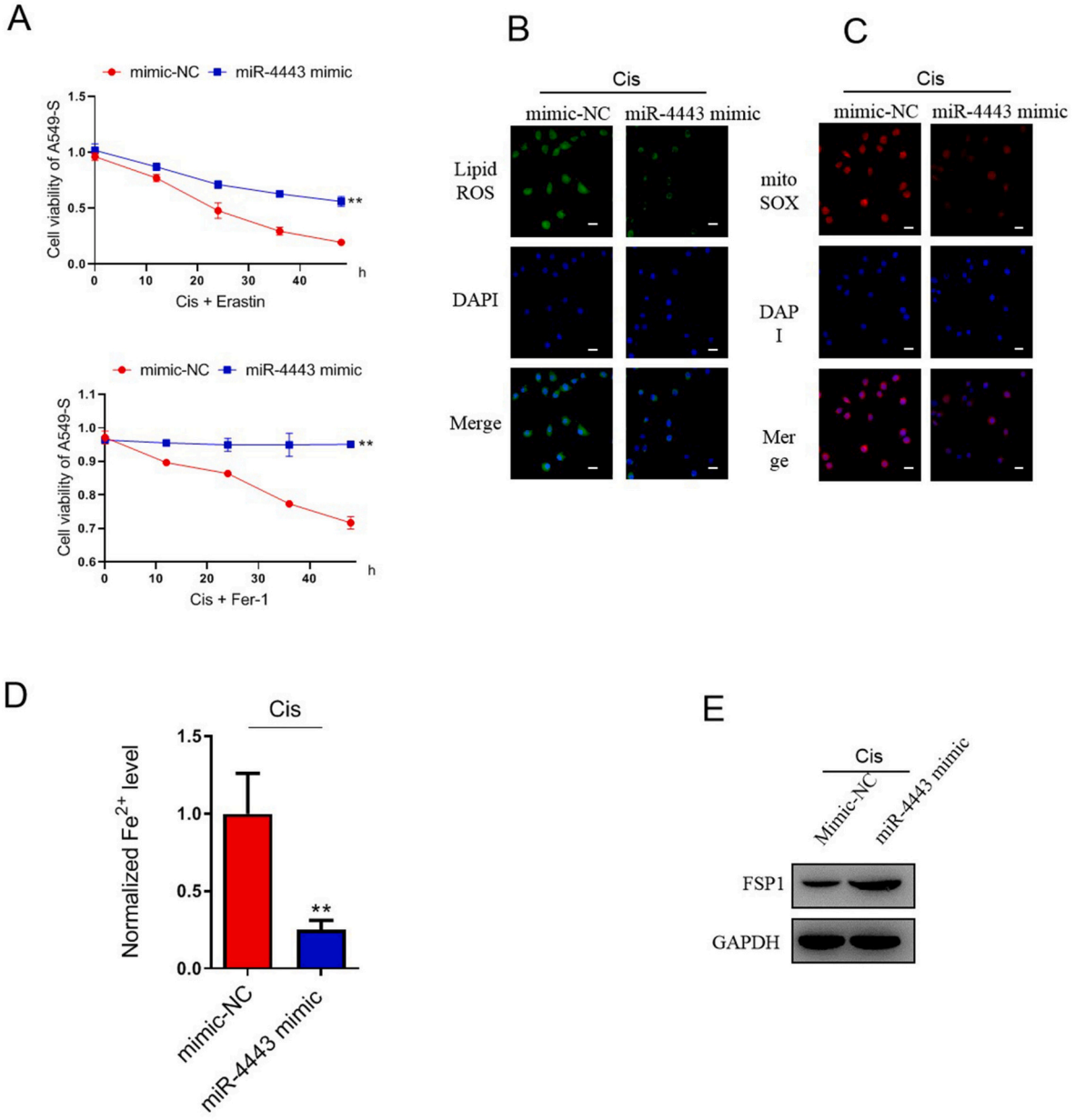

Fig. 4. miR-4443 alters cisplatin resistance of A549-S cells by suppressing ferroptosis. A. After transfection with mimic-NC or miR-4443 mimic, A549-S cells were exposed to cisplatin (5 μg/mL) and erastin (10 μmol/L) or Fer-1 (0.5 μmol/L) for 48 h. Cell viability was determined by CCK-8 assays. **p < 0.01 *vs.* the mimic-NC group. B, C and D. Lipid ROS levels, MitoSOX levels and iron accumulation in A549-S cells after different treatments were analyzed. Bar = 20 μm. **p < 0.01 *vs.* the cis + mimic-NC group. E. Representative blots showing the expression of FSP1 in A549-S cells transfected with mimic-NC or miR-4443 mimic upon cisplatin treatment are shown. Data are presented as the mean ± SD of three independent experiments.

this cisplatin-induced ferroptotic process.

3.4. miR-4443 promotes cisplatin resistance by suppressing ferroptosis

Next, to confirm the role of miR-4443 in cisplatin-induced ferroptosis, we transferred a miR-4443 mimic into A549-S cells subjected to the combination of cisplatin and erastin. CCK-8 assays revealed that the overexpression of miR-4443 increased A549-S cell viability compared with transfection with the mimic-NC (Fig. 4A). Interestingly, after treatment with both cisplatin and Fer-1, the cell viability of the miR-4443-enriched cells was still higher than that of the mimic-NC group, indicating that ferroptosis might not be the only pathway through which miR-4443 affects A549 resistance to cisplatin (Fig. 4A). We then analyzed lipid peroxidation and iron accumulation. As shown in Fig. 4B and C, the increased lipid ROS level and intracellular superoxide level induced by cisplatin treatment were suppressed by the overexpression of miR-4443. In addition, the upregulation of miRNA expression significantly reduced iron accumulation in A549-S cells upon cisplatin treatment (Fig. 4D). Furthermore, FSP1 expression was increased in the miR-4443-overexpressing cells compared with the mimic-NC-transfected cells (Fig. 4E).

3.5. miR-4443 regulates FSP1 m6A methylation

Methyltransferase-like 3 (METTL3), known as a methyltransferase that is responsible for N^6-methyladenosine (m^6A) methylation, was proven to participate in tumor resistance to cisplatin and NSCLC cell proliferation [28,29]. Based on bioinformatics analysis (www.targetscan.org), we found that METTL3 was a target gene of miR-4443 (Fig. 5A). For determination of whether METTL3 interacted with miR-4443 in cells, luciferase reporter vectors containing the wild-type (WT) or mutant (MUT) 3′-UTR of METTL3 were generated and transfected into HEK293T cells with upregulation or downregulation of miR-4443 expression. As shown in Fig. 5B, overexpression of miR-4443 markedly inhibited the luciferase activities of METTL3-WT, while inhibition of miR-4443 expression led to an increase in the luciferase activities of METTL3-WT but not those of the mutant, suggesting that METTL3 was a direct target of miR-4443. Next, we transfected miR-4443 into A549-S cells and miR-4443 inhibitor into A549-R cells to test the effect of miR-4443 on METTL3 expression. The results of western blotting demonstrated that METTL3 expression was decreased by miR-4443 transfection in A549-S cells and was increased when miR-4443 expression was inhibited in A549-R cells (Fig. 5C). However, the METTL3 mRNA levels were not affected by miR-4443 in these cells (Fig. 5D). In addition, we confirmed that METTL3 expression affected cell resistance to cisplatin using a CCK-8 assay. The transfection efficiencies of the METTL3-OE and METTL3-KD vectors were measured by qRT-PCR in these cells (Fig. 5E). Inhibition of METTL3 dramatically decreased the sensitivity of A549-S cells, whereas overexpression of METTL3 significantly sensitized A549-R cells to cisplatin (Fig. 5F).

Since METTL3 is a methyltransferase that carries out m6A methylation, we further explored whether m6A modification is involved in cisplatin-induced ferroptosis. The results showed that there was a 2-fold reduction in total m6A content in the miR-4443-overexpressing A549-S cells, while there was almost 2-fold enrichment in the miR-4443-silenced A549-R cells compared with the controls (Fig. 6A). FSP1 is a glutathione-independent ferroptosis suppressor [30]. Through bioinformatics analysis (http://m6avar.renlab.org/), we found five m6A sites with very high confidence at positions 2270, 2413, 4241, 4245 and 16,006 in *FSP1* mRNA, suggesting that the expression of FSP1 tended to be controlled by m6A modification (Fig. 6B). Subsequently, our data showed that decreased m6A enrichment of FSP1 and upregulated mRNA levels of FSP1 could be observed in the miR-4443 mimic-transfected A549-S cells. In contrast, m6A enrichment of FSP1 was increased and FSP1 mRNA expression was decreased in A549-R cells after treatment with the miR-4443 inhibitor (Fig. 6C). Consistently, overexpression of miR-4443 in A549-S cells inhibited METTL3 and enhanced FSP1 expression at the protein level, while silencing of miR-4443 suppressed FSP1 protein levels and upregulated METTL3 expression in A549-R cells (Fig. 6D). Additionally, transfection of the METTL3-KD vector enhanced both FSP1 mRNA and protein expression in A549-S cells compared with that of the control. Consistently, METTL3 overexpression markedly suppressed FSP1 expression at the mRNA and protein levels. Cotransfection with the FSP1-OE vector reversed the inhibitory effect of METTL3 in A549-R cells (Fig. 6E and F).

3.6. miR-4443 regulated cisplatin resistance through the METTL3/FSP1 pathway in vivo

To assess whether miR-4443 was an essential contributor to cisplatin resistance, we sought to determine whether overexpression of miR-4443 could reduce sensitivity to cisplatin *in vivo*. The mice injected with A549-S cells developed tumors resembling human NSCLC and were subjected to cisplatin treatment. Overexpression of miR-4443 abolished the inhibitory effect of cisplatin, resulting in a larger tumor size and weight than that of the mimic-NC-transfected tumors (Fig. 7A, B, and C). Consistently, in these tumor tissues from mice, a high level of miR-4443 inhibited tumor death caused by cisplatin by reducing the expression level of METTL3 and increasing the level of FSP1, which resulted in a higher expression level of the proliferation marker Ki-67 (Fig. 7D). Furthermore, we assessed the expression of FSP1 and METTL3 in clinical samples. As shown in Fig. 7E, a low METTL3 level and high FSP1 level were observed in the cisplatin-resistant tumor samples from patients, suggesting that miR-4443 played important roles in NSCLC resistance to cisplatin treatment *via* the METTL3/FSP1-mediated ferroptosis pathway.

4. Discussion

Resistance to cisplatin is still a major challenge in the treatment of NSCLC. As noted earlier, abundant evidence has shown that exosomes are a key mediator of resistance by transferring their contents. In this study, we compared the expression level of miR-4443 between exosomes derived from cisplatin-resistant and cisplatin-sensitive tumor tissues and cell lines. Further, we revealed the effect of miR-4443 on cisplatin resistance. Our findings indicated that the miR-4443 level was significantly upregulated in cisplatin-resistant tumor-released exosomes. Based on functional studies, we found that miR-4443 could be transferred to sensitive cells by exosomes and conferred chemoresistance in recipient cells. In addition, we confirmed that overexpression of miR-4443 in the sensitive cells reversed cisplatin-induced inhibition of viability, but knockdown of this miRNA in the resistant cells enhanced this effect. These data suggested that the expression of miR-4443 could regulate cellular sensitivity to cisplatin. Through bioinformatics analysis and luciferase assays, we found that METTL3 was a target gene of miR-4443. Further mechanistic analysis showed that miR-4443 regulated cell resistance to the expression of FSP1 in an m6A-dependent manner *via* METLL3.

Cisplatin is known to induce DNA lesions and activate programmed cell death, such as pyroptosis, apoptosis, and autophagy. Ferroptosis is a kind of iron- and oxidation-dependent death characterized by increased reactive oxygen species (ROS) and lipid peroxidation [31]. To date, ferroptosis is considered a novel process involved in the regulation of cell survival and death induced by cisplatin [32]. For example, researchers found that cisplatin treatment could also increase ROS levels and disrupt oxidative stress to induce cell death [33]. During this process, nuclear factor erythroid 2-related factor 2 and glutathione peroxidase 4 expression was inhibited in response to cisplatin [34,35]. In this study, we revealed that cisplatin led to low cell viability of A549-S cells, similar to erastin or RSL-3 treatment. Moreover, the inhibited cell viability caused by cisplatin could be partially reversed by apoptosis inhibitors and, more obviously, by ferroptosis inhibitors, indicating that

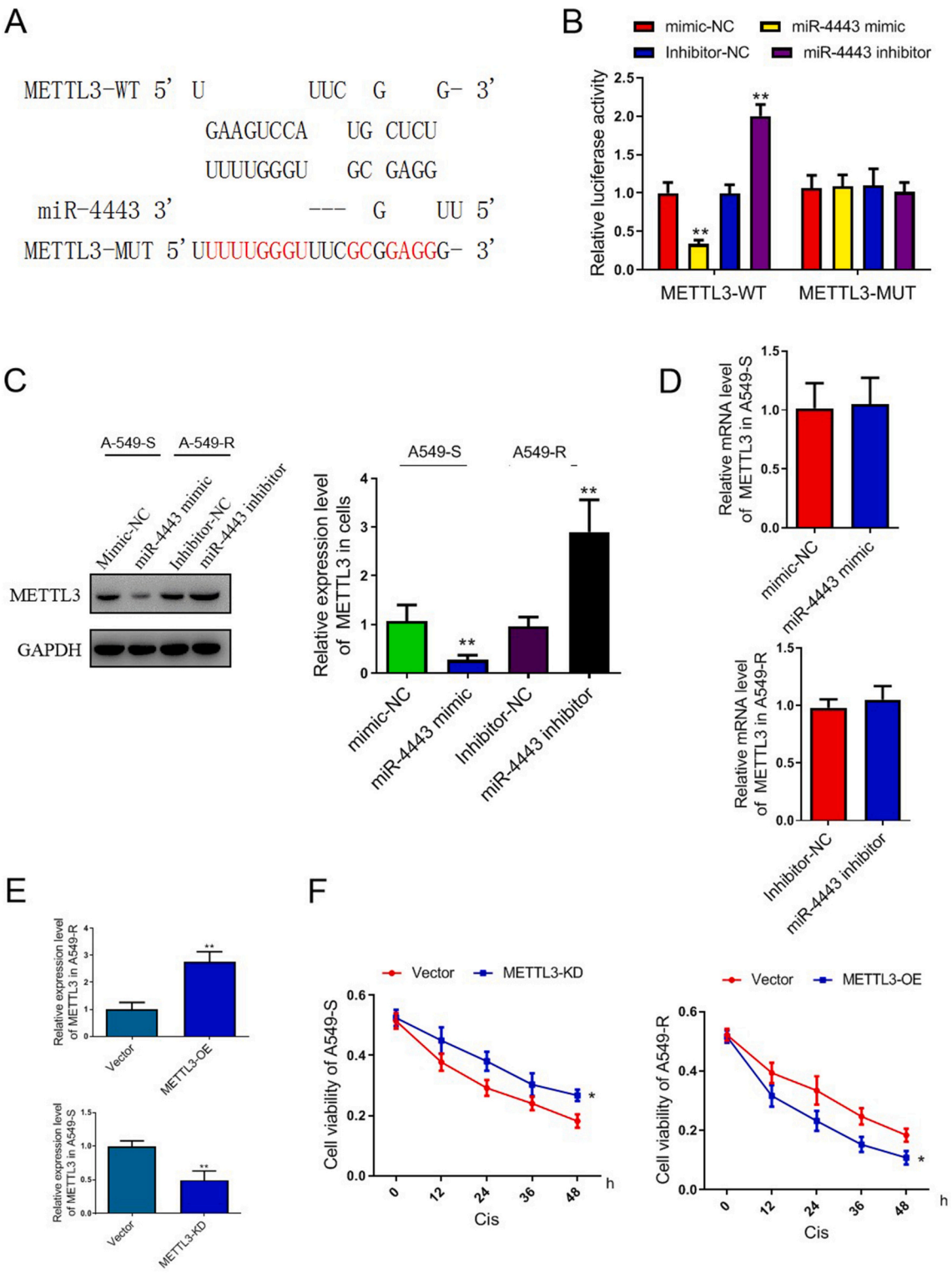

Fig. 5. METTL3 is a direct target of miR-4443. A. Putative targeting sequences of METTL3 and miR-4443 were predicted by the TargetScan database. B. Analysis of luciferase activity was performed in HEK293T cells cotransfected with miR-4443 mimic, inhibitor or related controls and METTL3-WT or METTL3-MUT vector. **p < 0.01 *vs.* the mimic-NC or inhibitor-NC group. C. Representative blots and analyses were performed for the expression of METTL3 in A549-S cells transfected with mimic-NC or miR-4443 mimic or in A549-R cells transfected with inhibitor-NC or miR-4443 inhibitor. **p < 0.01 *vs.* the mimic-NC or inhibitor-NC group. D. The mRNA expression of METTL3 in these cells after different transfections. E. After transfection with METTL3-OE, METTL3-KD or empty vector for 48 h, the level of METTL3 in the A549-S or A549-R cells was determined by qRT-PCR. F. After different transfections, the cells were subjected to cisplatin treatment for 0–48 h, and cell viability was assessed by CCK-8 assays. *p < 0.05, **p < 0.01 *vs.* the vector group. Data are presented as the mean ± SD of three independent experiments.

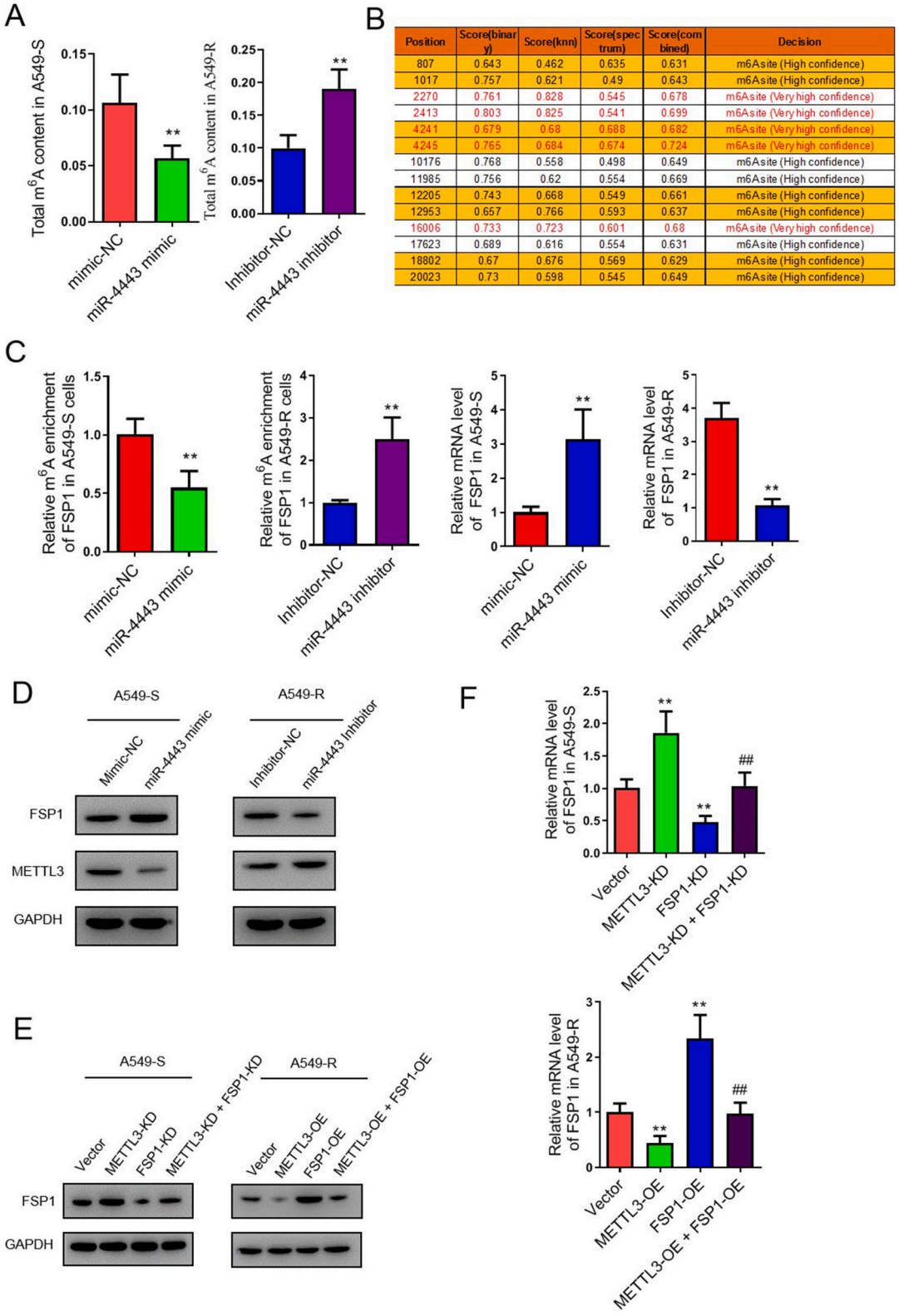

Position	Score(binary)	Score(knn)	Score(spectrum)	Score(combined)	Decision
807	0.643	0.462	0.635	0.631	m6Asite (High confidence)
1017	0.757	0.621	0.49	0.643	m6Asite (High confidence)
2270	0.761	0.828	0.545	0.678	m6Asite (Very high confidence)
2413	0.803	0.825	0.541	0.699	m6Asite (Very high confidence)
4241	0.679	0.68	0.688	0.682	m6Asite (Very high confidence)
4245	0.765	0.684	0.674	0.724	m6Asite (Very high confidence)
10176	0.768	0.558	0.498	0.649	m6Asite (High confidence)
11985	0.756	0.62	0.554	0.669	m6Asite (High confidence)
12205	0.743	0.668	0.549	0.661	m6Asite (High confidence)
12953	0.657	0.766	0.593	0.637	m6Asite (High confidence)
16006	0.733	0.723	0.601	0.68	m6Asite (Very high confidence)
17623	0.689	0.616	0.554	0.631	m6Asite (High confidence)
18802	0.67	0.676	0.569	0.629	m6Asite (High confidence)
20023	0.73	0.598	0.545	0.649	m6Asite (High confidence)

Fig. 6. miR-4443 regulates the m6A level of FSP1. A. The m6A methylation level of total RNA in A549-S and A549-R cells after different transfections. **p < 0.01 *vs.* the mimic-NC or inhibitor-NC group. B. The m6A methylation sites of *FSP1* were predicted, and the sites with high confidence are presented. C. The m6A methylation level and mRNA level of FSP1 in A549-S and A549-R cells after different transfections were detected by qRT-PCR. **p < 0.01 *vs.* the mimic-NC or inhibitor-NC group. D. Representative blots were performed for the expression of FSP1 and METTL3 in A549-S cells transfected with mimic-NC or miR-4443 mimic or in A549-R cells transfected with inhibitor-NC or miR-4443 inhibitor. E and F. After different transfections, the protein and mRNA levels of FSP1 in A549-S and A549-R cells were analyzed. **p < 0.01 *vs.* the vector group; ##p < 0.01 *vs.* the METTL3-KD- or METTL3-OE-transfected group. Data are presented as the mean ± SD of three independent experiments.

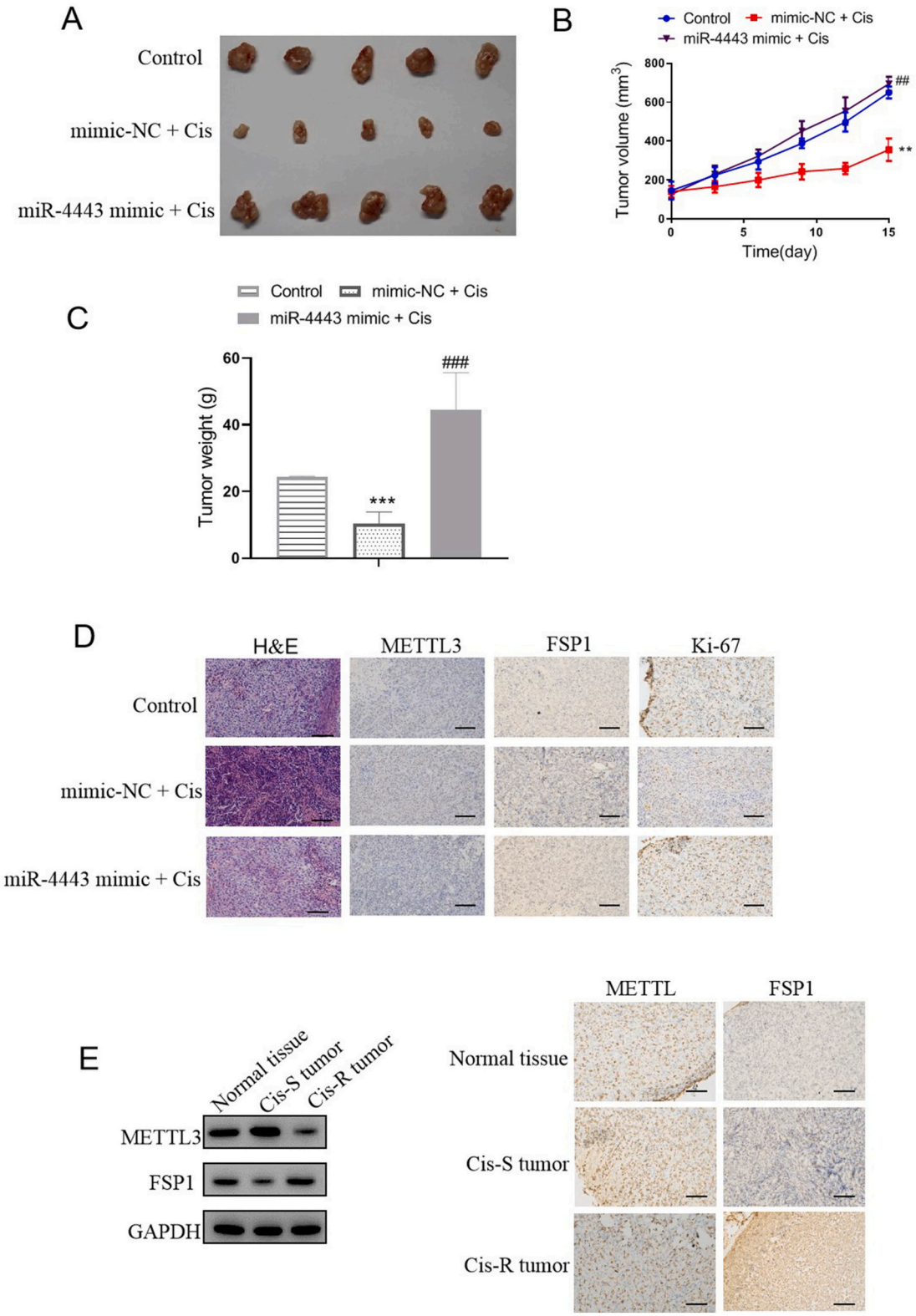

Fig. 7. miR-4443 regulates cisplatin resistance through the METTL3/FSP1 pathway *in vivo*. After transfection with mimic-NC or miR-4443 mimic, A549-S cells were injected subcutaneously into mice, followed by cisplatin treatment. The control group was injected with A549-S cells and treated with an equal volume of PBS. A. Typical photos of tumors from the control, cisplatin and miR-4443 mimic + cisplatin groups on day 15 after cisplatin administration. B and C. The tumor volume and weight of these groups. Data are presented as the mean ± SD for three mice of each group. $^{**}p < 0.01$, $^{***}p < 0.001$ *vs.* the control group; $\#\#p < 0.01$, $\#\#\#p < 0.001$ *vs.* the cisplatin + mimic-NC group. D. Representative images of H&E and IHC analysis of METTL3, FSP1 and Ki-67 in the tumor sections from these groups. Bar = 100 μm. E. Representative blots and IHC analysis were performed to determine the expression of METTL3 and FSP1 in cisplatin-resistant or cisplatin-sensitive tumors of patients. Bar = 100 μm.

ferroptosis is the main form of cell death caused by this chemical treatment. Cisplatin also induced ferrous iron and lipid ROS accumulation to activate the intracellular superoxide response in A549-S cells. The inhibition of ferroptosis *via* cotreatment with Fer-1 significantly abolished these effects. In addition, through western blot analysis, we found that cisplatin initiated ferroptosis by suppressing FSP1 [36]. To determine whether miR-4443 improves cancer cell drug resistance by inhibiting ferroptosis, we transferred miR-4443 to A549-S cells, followed by exposure to cisplatin combined with erastin or Fer-1. Overexpression of miR-4443 partially inhibited the potentiation of erastin in A549-S cells, while it enhanced the effect of Fer-1. In addition, miR-4443 inhibited key processes and markers of ferroptosis, including intracellular superoxide, ROS levels and ferrous iron production, and enhanced FSP1 expression in the cisplatin-exposed A549-S cells, indicating that the antiferroptotic effect of miR-4443 might be the reason for failure of cisplatin treatment.

Subsequently, we investigated the possible mechanism by which miR-4443 is involved in cisplatin-induced ferroptosis. Based on the bioinformatic analysis, we identified many miR-4443 target genes. Genes related to DNA repair, cell apoptosis, and cell ferroptosis ranked at the top of our list for further study. Since METTL3 is known to participate in cell resistance to cisplatin and NSCLC cell proliferation, we experimentally confirmed the interaction between miR-4443 and this gene using a luciferase assay. Moreover, METLL3 was proven to affect chemoresistance to cisplatin in A549 cells, which was consistent with previous studies [37,38]. METTL3, an essential N6-methyladenosine (m6A) methyltransferase, is involved in several biological processes, including chemoresistance [39,40], by facilitating mRNA biogenesis, decay and translation [41,42]. Jiang et al. revealed that m6A methylation regulated cell cycle functions to affect afatinib resistance in NSCLC [43]. *In vivo* data also found that FTO-dependent mRNA m6A hypomethylation was associated with enhanced tyrosine kinase inhibitor tolerance and led to a higher growth rate of tumors [44]. In the study of Dash et al., inhibition of m6A modification had a key role in cisplatin treatment failure in oral squamous cell carcinoma [45]. Here, we found that the high expression of miR-4443 decreased the m6A methylation level of FSP1 in A549-S cells, while silencing the expression of this microRNA increased the methylation of FSP1 in A549-R cells, suggesting that miR-4443 might confer cisplatin resistance by regulating METTL3-mediated m6A modification. Further, based on the bioinformatics analysis, five m6A sites with very high confidence were predicted in the mRNA of *SFP1*. Overexpression of miR-4443 in A549-S cells inhibited METTL3-induced m6A methylation and enhanced FSP1 expression at the mRNA and protein levels, whereas silencing of this microRNA had the opposite effect in A549-R cells. Gain- and loss-of-function analyses also confirmed that METTL3 negatively regulated FSP1 expression. Moreover, a similar trend of METTL3/FSP1 pathway expression was observed in our *in vivo* study using clinical samples. In summary, our present study found that high expression of miR-4443 negatively regulated METTL3-induced FSP1 m6A modification to inhibit cisplatin-induced ferroptosis and thus conferred cisplatin resistance in NSCLC.

MicroRNAs mainly regulate gene expression and are implicated in processes related to cisplatin resistance or sensitivity, such as cell cycle control, apoptosis, and DNA damage repair [46–48]. Therefore, miRNAs are not only used as chemoresistant markers but also as promising therapeutic agents to enhance lung cancer cell sensitivity. Deviations in the regulation of certain miRNAs may influence many mechanisms and hence contribute to chemo/radioresistance or chemo/radiosensitivity [49]. In this work, we showed that a high level of exosomal miR-4443 conferred cisplatin resistance in NSCLC *via* METTL3/FSP1-mediated ferroptosis. Our findings provide more in-depth insight into the chemoresistance of NSCLC and support a novel anticancer strategy by restoring METTL3/FSP1-mediated ferroptosis in tumor cells.

Supplementary data to this article can be found online at https://doi.org/10.1016/j.lfs.2021.119399.

Funding

This work was supported by the National Natural Science Foundation of China (Nos. 82002574).

Ethics declarations

This experiment was approved by the People's Hospital of Zhengzhou University, and written informed consent was obtained from all patients.

Consent for publication

Written informed consent for publication was obtained from all participants.

Data availability

The data used to support the findings of this study are available from the corresponding author upon request.

CRediT authorship contribution statement

Zhiyu Song and Gang Jia conceived the study. Zhiyu Song wrote the manuscript and designed the figures. Peizhi Ma and Shundong Cang contributed to the writing and editing of the manuscript. All authors and participants reviewed the paper and approved the final manuscript.

Declaration of competing interest

The authors declare that they have no conflicts of interest.

Acknowledgments

This work was supported by the National Natural Science Foundation of China (Nos. 82002574). We would like to thank all the researchers and study participants for their contributions.

References

[1] R.S. Herbst, D. Morgensztern, C. Boshoff, The biology and management of non-small cell lung cancer, Nature 553 (7689) (2018) 446–454.
[2] Z. Chen, C.M. Fillmore, P.S. Hammerman, C.F. Kim, K.K. Wong, Non-small-cell lung cancers: a heterogeneous set of diseases, Nat. Rev. Cancer 14 (8) (2014) 535–546.
[3] Gridelli C, Morabito A, Cavanna L, Luciani A, Maione P, Bonanno L, Filipazzi V, Leo S, Cinieri S, Ciardiello F et al: Cisplatin-based first-line treatment of elderly patients with advanced non-small-cell lung cancer: joint analysis of MILES-3 and MILES-4 phase III trials. J. Clin. Oncol. 2018, 36(25):2585–2592.
[4] J. Guo, B. Xu, Q. Han, H. Zhou, G. Wu, Ferroptosis: a novel anti-tumor action for cisplatin, Cancer Research & Treatment Official Journal of Korean Cancer Association 50 (2) (2017).
[5] F. Griesinger, E.E. Korol, S. Kayaniyil, N. Varol, T. Ebner, S.M. Goring, Efficacy and safety of first-line carboplatin-versus cisplatin-based chemotherapy for non-small cell lung cancer: a meta-analysis, Lung Cancer 135 (2019) 196–204.
[6] C. Zappa, S.A. Mousa, Non-small cell lung cancer: current treatment and future advances, Transl Lung Cancer Res 5 (3) (2016) 288–300.
[7] MacDonagh L, Gray SG, Breen E, Cuffe S, Finn SP, O'Byrne KJ, Barr MP: BBI608 inhibits cancer stemness and reverses cisplatin resistance in NSCLC. Cancer Lett. 2018, 428:117–126.
[8] T. Huang, C.X. Deng, Current progresses of exosomes as cancer diagnostic and prognostic biomarkers, Int. J. Biol. Sci. 15 (1) (2019) 1–11.
[9] D.K. Jeppesen, A.M. Fenix, J.L. Franklin, J.N. Higginbotham, Q. Zhang, L. J. Zimmerman, D.C. Liebler, J. Ping, Q. Liu, R. Evans, et al., Reassessment of exosome composition, Cell 177 (2) (2019) 428–445 (e418).
[10] P. Zheng, L. Chen, X. Yuan, Q. Luo, Y. Liu, G. Xie, Y. Ma, L. Shen, Exosomal transfer of tumor-associated macrophage-derived miR-21 confers cisplatin resistance in gastric cancer cells, J. Exp. Clin. Cancer Res. 36 (1) (2017), 53.
[11] K.B. Challagundla, P.M. Wise, P. Neviani, H. Chava, M. Murtadha, T. Xu, R. Kennedy, C. Ivan, X. Zhang, I. Vannini, et al., Exosome-mediated transfer of microRNAs within the tumor microenvironment and neuroblastoma resistance to chemotherapy, J. Natl. Cancer Inst. 107 (7) (2015).

[12] H. Zheng, Y. Zhan, S. Liu, J. Lu, J. Luo, J. Feng, S. Fan, The roles of tumor-derived exosomes in non-small cell lung cancer and their clinical implications, J. Exp. Clin. Cancer Res. 37 (1) (2018), 226.
[13] Wei F, Ma C, Zhou T, Dong X, Luo Q, Geng L, Ding L, Zhang Y, Zhang L, Li N et al: Exosomes derived from gemcitabine-resistant cells transfer malignant phenotypic traits via delivery of miRNA-222-3p. Mol. Cancer 2017, 16(1):132.
[14] Ma Y, Yuwen D, Chen J, Zheng B, Gao J, Fan M, Xue W, Wang Y, Li W, Shu Y et al: Exosomal transfer of cisplatin-induced miR-425-3p confers cisplatin resistance in NSCLC through activating autophagy. Int. J. Nanomedicine 2019, 14:8121–8132.
[15] S.O. Ebrahimi, S. Reiisi, Downregulation of miR-4443 and miR-5195-3p in ovarian cancer tissue contributes to metastasis and tumorigenesis, Arch. Gynecol. Obstet. 299 (5) (2019) 1453–1458.
[16] A. Meerson, H. Yehuda, Leptin and insulin up-regulate miR-4443 to suppress NCOA1 and TRAF4, and decrease the invasiveness of human colon cancer cells, BMC Cancer 16 (1) (2016), 882.
[17] M. Li, X. Zhang, X. Ding, Y. Zheng, H. Du, H. Li, H. Ji, Z. Wang, P. Jiao, X. Song, et al., Long noncoding RNA LINC00460 promotes cell progression by sponging miR-4443 in head and neck squamous cell carcinoma, Cell Transplant. 29 (2020), 963689720927405.
[18] Y. Gao, Y. Xu, J. Wang, X. Yang, L. Wen, J. Feng, lncRNA MNX1-AS1 promotes glioblastoma progression through inhibition of miR-4443, Oncol. Res. 27 (3) (2019) 341–347.
[19] Zhang W, Qiao B, Fan J: Overexpression of miR-4443 promotes the resistance of non-small cell lung cancer cells to epirubicin by targeting INPP4A and regulating the activation of JAK2/STAT3 pathway. Pharmazie 2018, 73(7):386–392.
[20] X. Qin, S. Yu, X. Xu, B. Shen, J. Feng, Comparative analysis of microRNA expression profiles between A549, A549/DDP and their respective exosomes, Oncotarget 8 (26) (2017) 42125–42135.
[21] Vella LJ, Scicluna BJ, Cheng L, Bawden EG, Masters CL, Ang CS, Willamson N, McLean C, Barnham KJ, Hill AF: A rigorous method to enrich for exosomes from brain tissue. J Extracell Vesicles 2017, 6(1):1348885.
[22] Rikkert LG, Nieuwland R, Terstappen L, Coumans FAW: Quality of extracellular vesicle images by transmission electron microscopy is operator and protocol dependent. J Extracell Vesicles 2019, 8(1):1555419.
[23] C. Zhang, D. Samanta, H. Lu, J.W. Bullen, H. Zhang, I. Chen, X. He, G.L. Semenza, Hypoxia induces the breast cancer stem cell phenotype by HIF-dependent and ALKBH5-mediated m(6)A-demethylation of NANOG mRNA, Proc. Natl. Acad. Sci. U. S. A. 113 (14) (2016) E2047–E2056.
[24] T. Song, Y. Yang, H. Wei, X. Xie, J. Lu, Q. Zeng, J. Peng, Y. Zhou, S. Jiang, J. Peng, Zfp217 mediates m6A mRNA methylation to orchestrate transcriptional and post-transcriptional regulation to promote adipogenic differentiation, Nucleic Acids Res. 47 (12) (2019) 6130–6144.
[25] C.C. Zhang, C.G. Li, Y.F. Wang, L.H. Xu, X.H. He, Q.Z. Zeng, C.Y. Zeng, F.Y. Mai, B. Hu, D.Y. Ouyang, Chemotherapeutic paclitaxel and cisplatin differentially induce pyroptosis in A549 lung cancer cells via caspase-3/GSDME activation, Apoptosis 24 (3–4) (2019) 312–325.
[26] Y. Zhang, X. Meng, C. Li, Z. Tan, X. Guo, Z. Zhang, T. Xi, MiR-9 enhances the sensitivity of A549 cells to cisplatin by inhibiting autophagy, Biotechnol. Lett. 39 (7) (2017) 959–966.
[27] L. Xiao, X. Lan, X. Shi, K. Zhao, D. Wang, X. Wang, F. Li, H. Huang, J. Liu, Cytoplasmic RAP1 mediates cisplatin resistance of non-small cell lung cancer, Cell Death Dis. 8 (5) (2017) e2803.
[28] M. Du, Y. Zhang, Y. Mao, J. Mou, J. Zhao, Q. Xue, D. Wang, J. Huang, S. Gao, Y. Gao, MiR-33a suppresses proliferation of NSCLC cells via targeting METTL3 mRNA, Biochemical & Biophysical Research Communications 482 (4) (2016) 582–589.
[29] S. Wang, P. Chai, R. Jia, R. Jia, Novel insights on m6A RNA methylation in tumorigenesis: a double-edged sword, Mol. Cancer 17 (1) (2018), 101.
[30] S. Doll, F.P. Freitas, R. Shah, M. Aldrovandi, M. Conrad, FSP1 is a glutathione-independent ferroptosis suppressor, Nature 575 (7784) (2019).
[31] S.J. Dixon, K.M. Lemberg, M.R. Lamprecht, R. Skouta, E.M. Zaitsev, C.E. Gleason, D.N. Patel, A.J. Bauer, A.M. Cantley, W.S. Yang, et al., Ferroptosis: an iron-dependent form of nonapoptotic cell death, Cell 149 (5) (2012) 1060–1072.
[32] J. Guo, B. Xu, Q. Han, H. Zhou, Y. Xia, C. Gong, X. Dai, Z. Li, G. Wu, Ferroptosis: a novel anti-tumor action for cisplatin, Cancer Res. Treat. 50 (2) (2018) 445–460.
[33] V.O. Kaminskyy, T. Piskunova, I.B. Zborovskaya, E.M. Tchevkina, B. Zhivotovsky, Suppression of basal autophagy reduces lung cancer cell proliferation and enhances caspase-dependent and -independent apoptosis by stimulating ROS formation, Autophagy 8 (7) (2012) 1032–1044.
[34] Q. Liu, K. Wang, The induction of ferroptosis by impairing STAT3/Nrf2/GPx4 signaling enhances the sensitivity of osteosarcoma cells to cisplatin, Cell Biol. Int. 43 (11) (2019) 1245–1256.
[35] Li Y, Yan H, Xu X, Liu H, Wu C, Zhao L: Erastin/sorafenib induces cisplatin-resistant non-small cell lung cancer cell ferroptosis through inhibition of the Nrf2/xCT pathway. Oncol. Lett. 2020, 19(1):323–333.
[36] S. Doll, F.P. Freitas, R. Shah, M. Aldrovandi, M.C. da Silva, I. Ingold, A. Goya Grocin, T.N. Xavier da Silva, E. Panzilius, C.H. Scheel, et al., FSP1 is a glutathione-independent ferroptosis suppressor, Nature 575 (7784) (2019) 693–698.
[37] M. Du, Y. Zhang, Y. Mao, J. Mou, J. Zhao, Q. Xue, D. Wang, J. Huang, S. Gao, Y. Gao, MiR-33a suppresses proliferation of NSCLC cells via targeting METTL3 mRNA, Biochem. Biophys. Res. Commun. 482 (4) (2017) 582–589.
[38] Wei W, Huo B, Shi X: miR-600 inhibits lung cancer via downregulating the expression of METTL3. Cancer Manag. Res. 2019, 11:1177–1187.
[39] D. Dai, H. Wang, L. Zhu, H. Jin, X. Wang, N6-methyladenosine links RNA metabolism to cancer progression, Cell Death Dis. 9 (2) (2018), 124.
[40] Liu Y, You Y, Lu Z, Yang J, Li P, Liu L, Xu H, Niu Y, Cao X: N (6)-methyladenosine RNA modification-mediated cellular metabolism rewiring inhibits viral replication. Science 2019, 365(6458):1171–1176.
[41] I. Barbieri, K. Tzelepis, L. Pandolfini, J. Shi, G. Millan-Zambrano, S.C. Robson, D. Aspris, V. Migliori, A.J. Bannister, N. Han, et al., Promoter-bound METTL3 maintains myeloid leukaemia by m(6)A-dependent translation control, Nature 552 (7683) (2017) 126–131.
[42] Zheng W, Dong X, Zhao Y, Wang S, Jiang H, Zhang M, Zheng X, Gu M: Multiple functions and mechanisms underlying the role of METTL3 in human cancers. Front. Oncol. 2019, 9:1403.
[43] Q. Meng, S. Wang, S. Zhou, H. Liu, X. Ma, X. Zhou, H. Liu, C. Xu, W. Jiang, Dissecting the m(6)A methylation affection on afatinib resistance in non-small cell lung cancer, Pharmacogenomics J 20 (2) (2020) 227–234.
[44] F. Yan, A. Al-Kali, Z. Zhang, J. Liu, J. Pang, N. Zhao, C. He, M.R. Litzow, S. Liu, A dynamic N(6)-methyladenosine methylome regulates intrinsic and acquired resistance to tyrosine kinase inhibitors, Cell Res. 28 (11) (2018) 1062–1076.
[45] O. Shriwas, M. Priyadarshini, S.K. Samal, R. Rath, S. Panda, S.K. Das Majumdar, D. K. Muduly, M. Botlagunta, R. Dash, DDX3 modulates cisplatin resistance in OSCC through ALKBH5-mediated m(6)A-demethylation of FOXM1 and NANOG, Apoptosis 25 (3–4) (2020) 233–246.
[46] P. Ceppi, G. Mudduluru, R. Kumarswamy, I. Rapa, H. Allgayer, Loss of miR-200c expression induces an aggressive, invasive, and chemoresistant phenotype in non-small cell lung cancer, Mol. Cancer Res. 8 (9) (2010) 1207–1216.
[47] Yuwen DL, Sheng BB, Liu J, Wenyu W, Shu YQ: MiR-146a-5p level in serum exosomes predicts therapeutic effect of cisplatin in non-small cell lung cancer. European Review for Medical & Pharmacological Sciences 2017.
[48] G. Zhuang, X. Wu, Z. Jiang, I. Kasman, J. Yao, Tumour-secreted miR-9 promotes endothelial cell migration and angiogenesis by activating the JAK-STAT pathway, EMBO J. 31 (17) (2012) 3513–3523.
[49] Florczuk M, Szpechcinski A, Chorostowska-Wynimko J: miRNAs as biomarkers and therapeutic targets in non-small cell lung cancer: current perspectives. Target. Oncol. 2017, 12(2):1–22.